JOURNAL OF PROPULSION AND POWER
Vol. 9, No. 4, July–Aug. 1993

Design Verification of Ground Run-Up Noise Suppressors for Afterburning Engines

S. A. Fisher* and A. M. Abdel-Fattah†
DSTO Aeronautical Research Laboratory, Melbourne, Australia
and
L. A. Challis‡
Challis and Associates Pty., Ltd., Sydney, Australia

New facilities for ground running of engines in Royal Australian Air Force F/A-18 aircraft feature air-cooled exhaust augmentors for noise suppression. Aerothermodynamic aspects of the augmentor designs were appraised in some detail, making use of isothermal scale model tests, ejector theory, and available empirical data. Quantitative assessments were made of cooling flow pumping performance, and geometric features were identified which are important to the symmetry of the flow in the augmentor ducts. The final designs displayed satisfactory aerodynamic behavior, tolerant to both inlet asymmetries and reasonable levels of engine jet misalignment. The estimated pumping performance exceeded the design requirements.

Nomenclature

A = local flow area
C_p = specific heat at constant pressure
d = diameter of primary augmentor tube, uninstalled engine facility
H = enthalpy
h = height of primary augmentor tube, installed engine facility
I = momentum
J = stream thrust
k = pressure loss coefficient
l = length of primary augmentor tube
M = Mach number
m = mass flow rate
P = static pressure
P_0 = total pressure
R = gas constant
T = total temperature
w = width of primary augmentor tube, installed engine facility
γ = ratio of specific heats
μ = augmentation ratio m''/m'
ν = augmentor main duct area/nozzle throat area

Subscripts
a = ambient conditions
1 = entry plane of augmentor duct
2 = exit plane of augmentor duct

Superscripts
$'$ = jet flow
$''$ = entrained flow

Introduction

FOR effective suppression of exhaust noise in jet engine run-up facilities, the high-velocity exhaust jets must be enclosed and treated in such a way that the engine and jet noise are absorbed, and that the velocity of the final suppressor efflux is sufficiently low for its noise level to be acceptable. This can be readily achieved with the introduction of water, but with attendant penalties which include high capital and operating costs, structural corrosion, and environmental problems. Modern facilities are generally air-cooled, using exhaust augmentors to enclose the hot, high-velocity jets and entrain atmospheric air for cooling and noise suppression.

Exhaust augmentors for afterburning engines are subject to very high levels of input energy flux, and require effective integration of aerothermodynamic, acoustic, and structural design technologies for successful, long-life operation. In particular, satisfactory internal aerodynamic performance and behavior are critical to their operational effectiveness and durability. Not only must an augmentor pump sufficient cooling air to reduce the final mixed flow velocity and temperature to acceptable levels, but the flow within the augmentor must be stable, with no danger of direct impingement of uncooled exhaust gases on the duct walls. Any tendency towards instability or asymmetry of the internal flow may cause overheating, excessive aerodynamic loading, and premature structural failure.

New facilities have been built for ground running of the General Electric F404 engines which power Royal Australian Air Force F/A-18 aircraft. Provision is made for running both uninstalled engines mounted on a test stand, and engines installed in aircraft, at up to full afterburning power. Before final commitment to the designs, the prospective aerothermodynamic behavior of the exhaust augmentors was examined in some detail to minimize the risks outlined above. A comprehensive report on the appraisal is presented in Ref. 1; it did not address acoustic, structural, or material aspects of the designs.

Facility Layout

Separate facilities are provided for installed and uninstalled engine testing. They are shown in outline, together with leading dimensions, in Figs. 1 and 2, respectively. The main augmentor ducts are rectilinear in cross section, and are lined internally with acoustic absorbent panels. Deflector ramps are fitted to the duct exits to minimize exhaust blast effects at ground level and for added acoustic attenuation.

Each duct is equipped with an air inlet arrangement designed to limit the flow velocity in the immediate vicinity of

Received Feb. 20, 1991; revision received Dec. 15, 1992; accepted for publication Jan. 6, 1993.

*Head of Propulsion, 506 Lorimer Street, Fishermens Bend, Vic 3207.
†Senior Research Scientist, 506 Lorimer Street, Fishermens Bend, Vic 3207.
‡Director, P.O. Box 199, Kings Cross, NSW 2011.

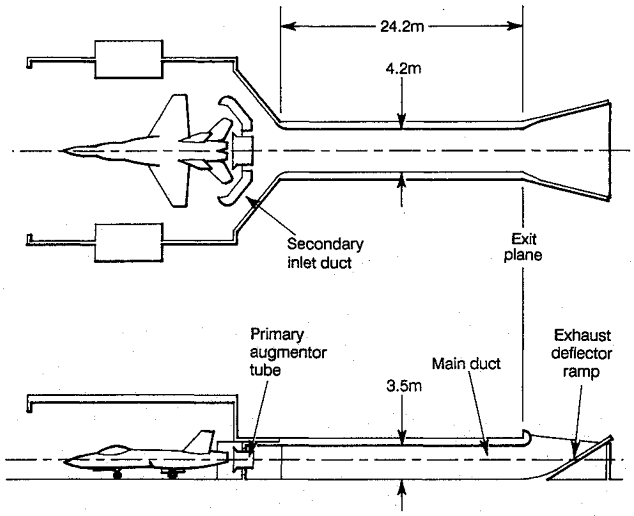

Fig. 1 Installed engine test facility.

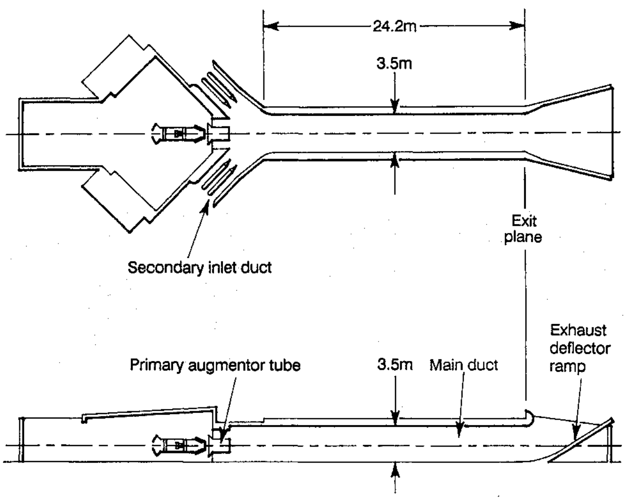

Fig. 2 Uninstalled engine test facility.

the test aircraft or engine. The engine exhaust jets are introduced to the ducts by way of primary augmentor tubes, of circular cross section in the case of the uninstalled engine facility, and of compound rectangular-circular cross section to match the aircraft's twin exhaust nozzle configuration in the installed engine facility. Part of the cooling air is introduced through these primary tubes, but most enters through the larger secondary inlets.

The installed engine facility is designed to accommodate two engines operating simultaneously at up to intermediate rated power (IRP) (equivalent to maximum dry or military power), or one engine in maximum afterburner (max AB) mode with the second engine either shut down or at idle condition.

Assessment of Pumping Performance

Theoretical Approach

Ejector theory using compressible flow relationships based on principles of conservation of mass, momentum, and energy may be used to calculate rates of entrainment of cooling air in an augmentor duct. The basic theory uses one-dimensional flow relationships with no friction losses, treating the flow at the duct exit as fully mixed and uniform. Losses in various parts of the duct, such as the entrained (secondary) flow inlet system, the duct walls, and the exhaust stack, may be accounted for with appropriate pressure drop coefficients, and the effect of incomplete mixing between the jet and the en-

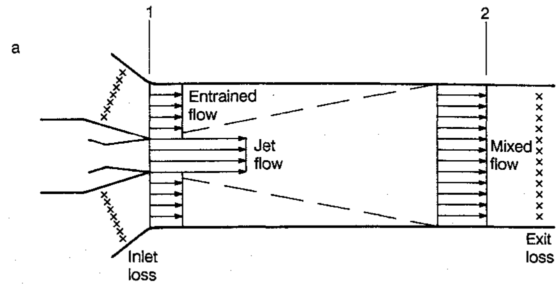

Fig. 3 Simplified ejector model.

trained flow within the duct may also be accommodated if the nonuniform distributions of velocity, temperature, and gas properties are known.[2]

In the present exercise, theoretical calculations were used mainly to provide a framework against which empirical data could be assessed, and to facilitate interpretation of isothermal model test results. The simplified flow model adopted for this purpose is shown in Fig. 3. Departures from idealized conditions were accommodated by the application of two variable loss coefficients, k_1 and k_2, defined as follows:

$$k_1 = 2(P_a - P_1)/P_1\gamma_1 M_1^2 - 1 \tag{1}$$

$$k_2 = 2(P_2 - P_a)/P_2\gamma_2 M_2^2 \tag{2}$$

Notional pressure losses were thus imposed at the secondary flow inlet system and the augmentor duct exit, and it was implied that the effects of all losses, including wall friction, could be lumped into these two coefficients. The effect of incomplete mixing in the augmentor ducts was not expected to be sufficient to warrant specific treatment. According to experience,[3,4] the pumping performance of installations of this type becomes relatively insensitive to augmentor duct length when the ratio of length to hydraulic diameter is greater than about four; this suggests that the kinetic and thermal mixing which occurs downstream of four hydraulic diameters has little impact on the augmentation ratio. Evidence from model tests, described below, shows that kinetic mixing with isothermal flow is actually far from complete at four hydraulic diameters. However, the designs of present interest had length-to-hydraulic diameter ratios in excess of six, dictated by acoustic considerations. Moreover, increased rates of mixing are known to occur in ejectors when the jet temperature is increased.[2,5]

The relationships used in the theoretical treatment, referring to the flow stations in Fig. 3, were as follows:

Conservation of mass

$$m_2 = m_1' + m_1'' \tag{3}$$

where

$$m = PAM\sqrt{[1 + (\gamma - 1)M^2/2]\gamma/RT} \tag{4}$$

Conservation of momentum

$$J_2 = J_1' + J_1'' \tag{5}$$

where

$$J = PA(1 + \gamma M^2) \tag{6}$$

Conservation of energy

$$H_2 = H_1' + H_1'' \tag{7}$$

where

$$H = mC_pT \tag{8}$$

Pressure balance

$$P_1'' = P_a/[1 + (1 + k_1)\gamma_1'' M_1''^2/2] \tag{9}$$

$$P_2 = P_a/(1 - k_2\gamma_2 M_2^2/2) \tag{10}$$

The solution of the equations and procedure for calculating augmentor performance are fully described in Ref. 6.

In Fig. 4 theoretical curves of augmentation ratio are plotted against augmentor duct area ratio for single-engine, max AB operation, this being the condition which imposes the greatest thermal loading on the augmentor duct. Curves are shown for four different combinations of the two loss coefficients k_1 and k_2, the relatively high maximum value of 2.5 assigned to k_2 being chosen to ensure that the effect of more complex exhaust stack arrangements would be spanned by the calculations. The figures used for air and fuel mass flow, exhaust temperature and pressure, nozzle configuration, and exhaust gas properties for the F404 engine were all based on Ref. 7. The effect of a second engine operating at idle power was ignored. The effect of the primary augmentor tube was also ignored to avoid the use of the more complex two-stage ejector theory.[6] This was well justified in the light of subsequent model tests (described below) which showed that the primary tube needed to be reduced to vestigial proportions to achieve acceptable flow behavior.

Comparison with Empirical Data

Superimposed on the theoretical curves in Figs. 4 and 5 are data based on correlations of scale model test results relating to operational facilities.[4,8] A point representing the design performance of an installation used for testing F404 engines in CF-18 aircraft[9] is also included. Notwithstanding the wide possible variation in augmentor designs and the corresponding possible variation in effective loss characteristics, the trends exhibited by these empirical data, all of which are reported to have been validated to some degree by full-scale measurement, bear a quite consistent relationship to the theoretical curves. Additional points shown in Fig. 4 relate to the model tests described below, and are discussed later.

Figure 4 includes a vertical scale of fully mixed exhaust gas temperature, which is directly related to the augmentation ratio. The figure indicates that, for any reasonable level of aerodynamic losses, the duct components should be exposed to temperatures no higher than about 300°C, well below the level of tolerance for the materials used. This, of course, assumes that the flow in the augmentor ducts is well behaved, with no tendency for the uncooled jets to impinge on the duct walls. The use of rectilinear (as distinct from, e.g., circular)

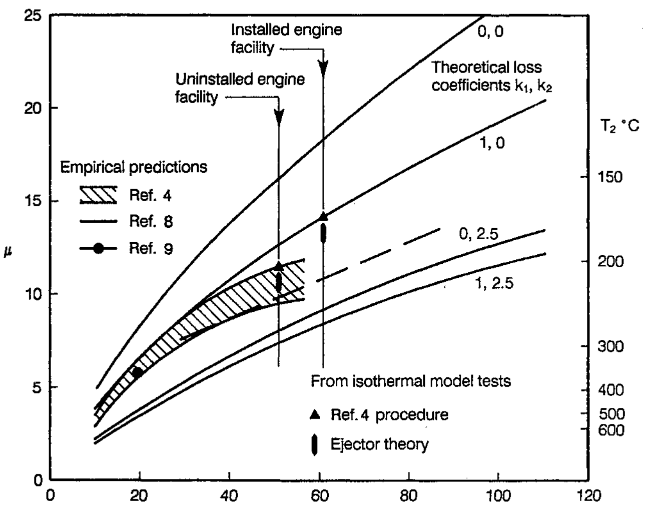

Fig. 4 Pumping performance—one engine, max AB.

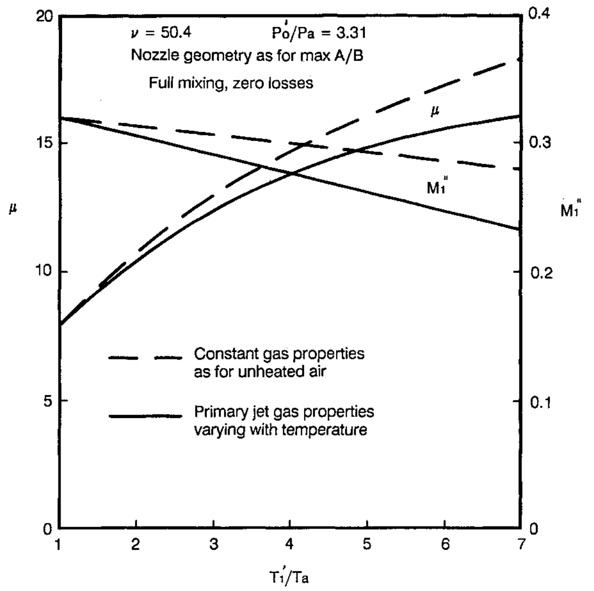

Fig. 5 Theoretical effect of jet temperature and gas properties.

duct cross sections probably also calls for conservative interpretation of Fig. 4.

Model Tests

Purpose

Aerodynamic testing of scale models of the two facilities was undertaken to establish that the augmentor internal flow was not likely to behave in such a way as to cause excessive local thermal or aerodynamic loading, to confirm the predicted levels of pumping performance, to optimize detailed aspects of the aerodynamic designs, and to assess the tolerance of the internal flow to inlet asymmetry and jet misalignment.

Model Design

Models representing the two facilities were built to $\frac{1}{45}$ scale, reproducing the internal geometries of the exhaust augmentors, but not detailed internal surface features such as perforated acoustic linings. The engine exhaust jet was simulated with unheated, pressurized air issuing from a convergent-divergent nozzle of correct geometrical scale. All tests were arranged to represent single-engine, max AB operation, since this was the critical case governing the thermal design, and also the condition thought more likely to lead to problems with flow asymmetry in the installed engine augmentor.

Flow Scaling

The implications of using unheated air to simulate the engine exhaust jet could not be overlooked. The entrainment properties of a jet, in a one-dimensional sense, are generally regarded as being a function of jet momentum.[4] If this were wholly the case, then a compressible jet with a given pressure ratio and fixed gas properties, issuing from a nozzle of fixed dimensions, would entrain flow at a rate which is independent of its temperature, because jet momentum

$$I = PA\gamma M^2 \tag{11}$$

is independent of temperature. This is not sustained by one-dimensional ejector theory. Figure 5, which contains curves calculated for an idealized ejector geometry equivalent to the uninstalled engine augmentor in Fig. 2, shows that an increase in jet temperature ratio from 1 to 7 (equivalent to transition from isothermal conditions to max AB jet temperature), with constant gas properties, theoretically results in a reduction in entrained airflow at loss-free conditions which corresponds to a reduction in entrained flow inlet Mach number of some

11%. When the appropriate variation of gas properties resulting from the combustion process is superimposed on the temperature increase, the reduction in entrained flow inlet Mach number becomes about 27%.

It would be possible to adjust the size, pressure, and/or Mach number of the unheated model jet to compensate for these effects. However, this was not justified when complete simulation would remain unattainable with the isothermal flow. The simpler approach, adhering to geometric similarity with the correct jet pressure ratio, was adopted. To simulate max AB operation, this required a nozzle blowing pressure of 340 kPa. The augmentation ratios measured in the isothermal models could be translated to the full-scale, hot jet situation with reasonable confidence, as will be seen below.

Only loose simulation of the three-dimensional mixing flows in the full-scale augmentor ducts was possible with the cold air jet. Lower rates of mixing could be expected because of the reduced density differentials,[10] and the gas velocities were different. Nevertheless, the measured pressure and mean velocity distributions could be expected to be qualitatively similar to the full-scale distributions, notably in respect of any asymmetrical flow behavior.

Nozzle Alignment

The two engines in the F/A-18 aircraft are installed with their exhaust nozzle centerlines laterally spaced 0.9-m apart and canted inwards with an included angle of about 4 deg. In the normal arrangement representing single-engine operation in the installed engine model, the single nozzle was therefore displaced laterally 0.45-m (note that all dimensions quoted relate to full-scale facilities) from the duct centerline and angled 2-deg towards the centerline. The exit plane of the nozzle was normally positioned 1.4-m upstream of the commencement of the throat of the primary augmentor tube, and in the vertical plane the nozzle axis was placed on and parallel to the duct centerline. This arrangement is shown in plan view in Fig. 6. For investigative purposes, some tests were conducted with different arrangements from that shown.

In the uninstalled engine model, the nozzle axis was positioned on and parallel to the duct centerline, with the same lengthwise spacing as that shown in Fig. 6.

Measurements and Observations

Air velocity measurements were made using a traversing pitot-static tube aligned with the duct axis, both in the exit planes of the main ducts as defined in Figs. 1 and 2 and at intermediate flow stations approximately two duct heights further upstream. Wall static pressure distributions were measured with flush tappings, and flow visualization was carried out with both schlieren apparatus and wool tufts. The tests are fully reported elsewhere,[1] and only selected results are presented here.

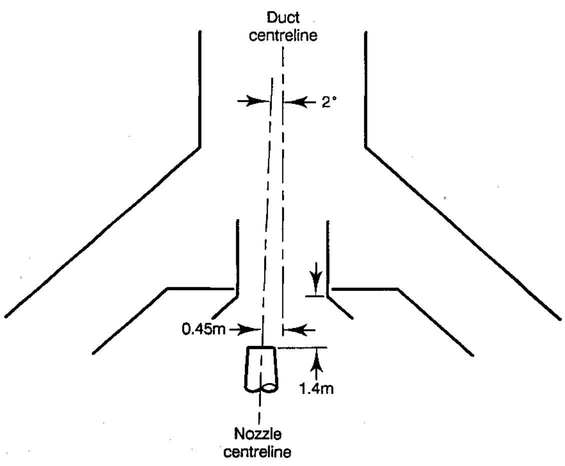

Fig. 6 Normal nozzle alignment in installed engine model.

Effect of Primary Augmentor Tube Geometry

In early tests with a relatively long and narrow primary augmentor tube in the installed engine facility model, unacceptable distortion was observed in the augmentor duct flow. This is illustrated in Fig. 7, which shows how the velocity distributions at both the intermediate and exit flow stations varied as the jet nozzle alignment was changed from coaxial, through simple lateral displacement, to the "normal" combination of lateral and angular displacement defined in Fig. 6. Each velocity map includes an indication of the local position of the projection of the nozzle axis; as can be seen, lateral displacement of the jet had an exaggerated effect on the distortion of the downstream flow, relative to that which may have been expected on the basis of simple projection of the jet axis. The local peak velocity (and, by implication, the local peak temperature in the case of a hot jet) was increased, as was the risk of hot gas impingement on the duct lining.

This was caused by interaction between the jet and the primary augmentor tube. When the jet was displaced laterally from a coaxial position, it tended to become attached to the nearer wall of the primary tube by a mechanism akin to the Coanda effect, and was therefore diverted further in the direction of the original lateral displacement, negating the otherwise beneficial effect of the 2-deg cant of the nozzle axis back towards the duct centerline. In addition to the adverse effect of the resulting asymmetrical flow in the main augmentor duct, in a full-scale facility this would cause significant (probably unsteady) lateral force on the primary tube structure, as well as heat exposure of the tube wall. The nature of the phenomenon is revealed in the schlieren photograph in Fig. 8, showing the asymmetrically disposed jet being deflected in its passage through an isolated augmentor tube. The tube in the photograph is of compound rectangular/circular

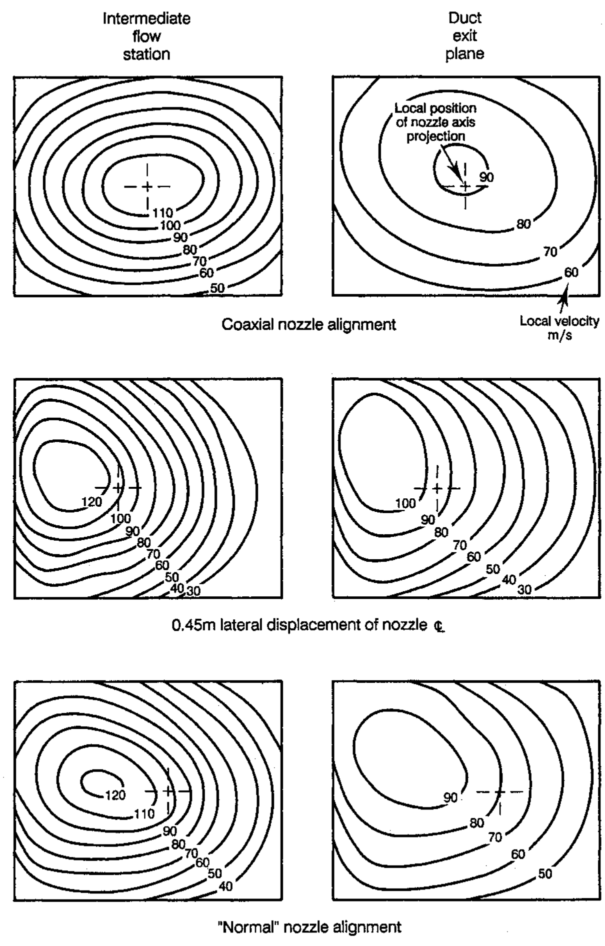

Fig. 7 Effect of jet alignment on velocity distribution—installed engine facility, w = 2.2 m, h = 1.3 m, l = 2.0 m.

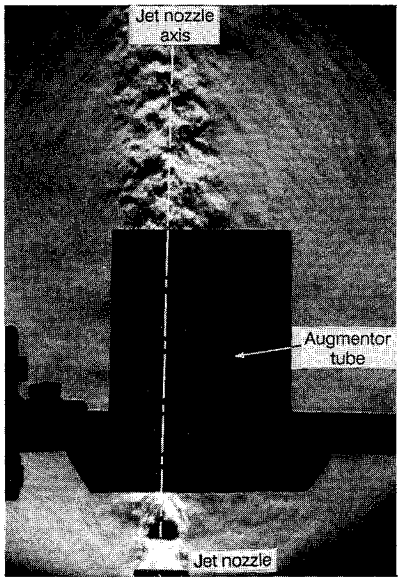

Fig. 8 Jet-primary tube interaction.

cross section, as used in the installed engine test facility, viewed normal to its major axis.

The effect of primary tube geometry on the magnitude of this effect was investigated by varying the length, overall scale, and aspect ratio of the tube. Figure 9 shows velocity profiles measured on the midheight horizontal plane at the exit of the main augmentor duct, with normal (asymmetrical) jet alignment, and with four different lengths of primary tube of 1.5 × 2.4 m compound cross section. For all but the very shortest tube, the lateral location of the peak velocity at the main duct exit was displaced a significant distance from the projection of the nozzle centerline. On this basis, a primary tube was adopted for the installed engine augmentor with a length of 1.3 m and a compound cross section of 1.5 × 2.4 m. With this configuration the jet/tube interaction was arguably favorable since, on the evidence of Fig. 9, the 1.3-m-long tube deflected the jet core from the projection of the nozzle axis by a small degree so that it became approximately centralized at the main duct exit.

Consistent with the above, a primary tube 1.3-m in diameter and 1.2-m long was adopted for the uninstalled engine facility. Although the uninstalled engine, mounted on its test stand, should always be aligned coaxially, the symmetry of the main duct flow was found to be quite sensitive with longer primary tubes. In both cases there was a measurable but otherwise insignificant reduction in mass augmentation ratio associated with adoption of these short primary tubes, relative to the longer tubes originally proposed.

Inlet and Exit Geometry Refinements

By means of flow visualization and pressure measurement, a number of geometrical features were identified which threatened to impair the flow symmetry and/or diminished the cooling flow pumping performance. Investigation of these features led to the adoption of refinements in the vicinity of the main duct inlets and exits of both the installed and uninstalled engine facilities, as follows:

1) The feet of the exhaust deflector ramps were displaced downstream of the main duct exit planes by one-half of a duct height, to relieve their back-pressurization effect, increase the cooling flow, and reduce the flow distortion at the exit planes.

2) Bellmouth fairings were added to the secondary inlets of both augmentor ducts, and the vertical corners where the secondary inlet ducts were integrated with the main ducts were also faired to control flow separations at these locations.

Figures 10 and 11 show the velocity distributions measured at the exit planes of the two models, following incorporation

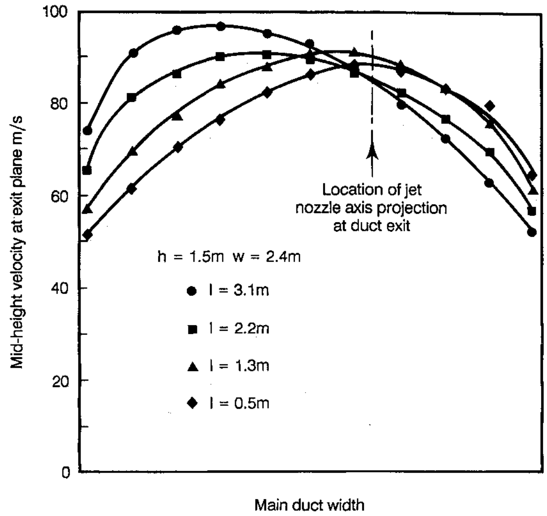

Fig. 9 Effect of primary tube length on main duct velocity profile—installed engine facility.

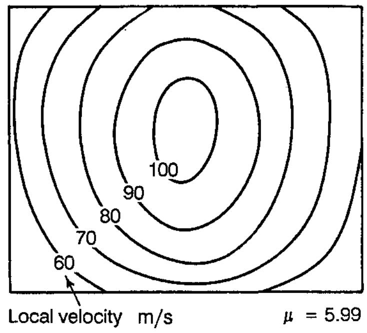

Fig. 10 Exit velocity distribution—installed engine facility.

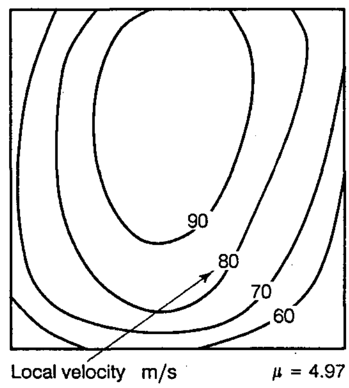

Fig. 11 Exit velocity distribution—uninstalled engine facility.

of the above refinements. In both cases the flow was symmetrical in the lateral plane, while exhibiting some residual distortion in the vertical plane due to the upstream influence of the exhaust deflector ramps. The isothermal augmentation ratios, determined by integrating the measured duct exit velocities, were 5.99 and 4.97 for the installed and uninstalled engine testing facilities, respectively.

Sensitivity to Inlet Disturbances

Because the two secondary flow inlets in the uninstalled engine facility were open to the elements, the possibility of partial blockage of one of the inlets, e.g., by blown debris, could not be overlooked. To gain a measure of the sensitivity of the augmentor flow to such an occurrence, tests were conducted with one of the three passages between the acoustic splitters blocked, on each side in turn, as indicated in Fig. 12. The augmentor geometry was an early one which included

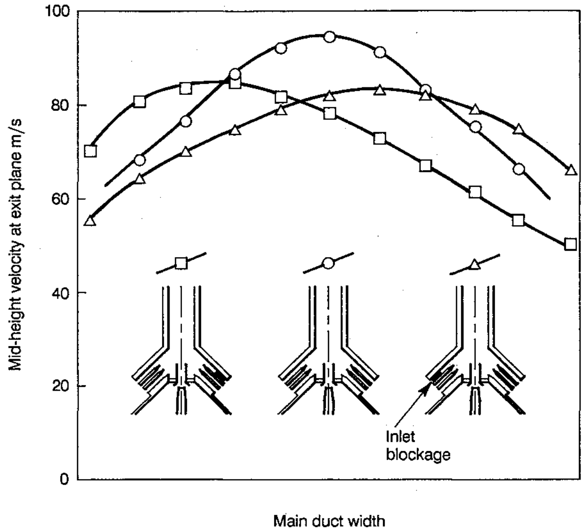

Fig. 12 Effect of asymmetrical inlet blockage.

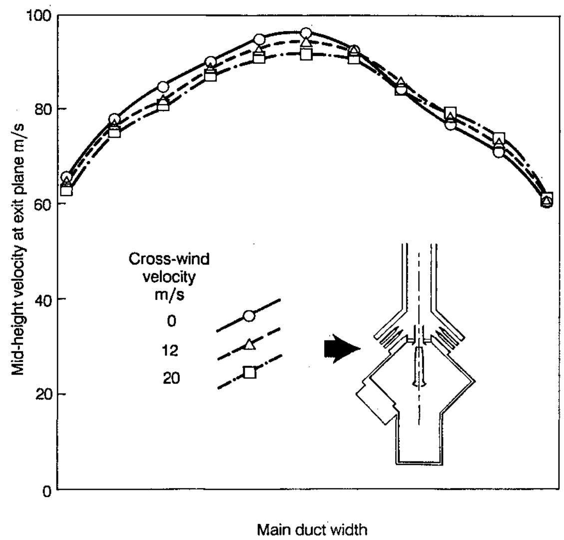

Fig. 13 Effect of crosswind.

none of the refinements discussed above, but the results were qualitatively valid.

The graph in Fig. 12 shows the midheight exit velocity profiles for the two asymmetrical conditions compared with the profile measured with the normal symmetrical arrangement. The resulting levels of distortion, while far from desirable, demonstrated reasonable tolerance to inlet asymmetry in view of the extreme nature of the blockages involved.

The uninstalled engine facility was arguably also vulnerable to the effect of crosswinds on the secondary inlet flow. The model was tested with wind velocities up to 20 m/s normal to the augmentor centerline, directed at one of the secondary inlets, with the results shown in Fig. 13. The effect of the crosswind on the symmetry of the duct flow was insignificant, which was perhaps not surprising in view of the fact that even the highest wind velocity was small relative to the local velocity of the entrained air at the secondary inlets. While the evidence was again qualitative, it indicated that the adverse effect of crosswind could be discounted.

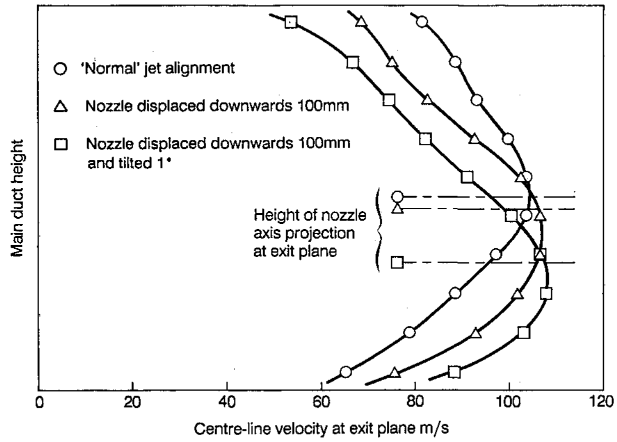

Fig. 14 Effect of jet misalignment.

Sensitivity to Jet Misalignment

Tests were carried out to determine the sensitivity of the augmentor flow to jet misalignment in the vertical plane. Here, the main focus of concern was the installed engine facility because, although means were to be provided for adjustment and restraint of the test aircraft attitude, some variation of undercarriage geometry might be expected both between different aircraft and, with a given aircraft, during engine thrust excursions. The tests were conducted with the fully refined model configuration.

Figure 14 compares velocity profiles measured on the vertical centerline at the duct exit plane with 1) normal jet alignment; 2) the jet parallel to the augmentor centerline but displaced downwards by 100 mm (full scale); and 3) the nozzle displaced downwards by 100 mm, and also tilted downwards by an angle (approximately 1 deg) which would apply had the 100-mm displacement been caused by rotation of the aircraft about its main undercarriage.

These displacements were more than double the maximum movement which had been measured on a restrained aircraft during a trial engine run with extreme power excursions.

For each case, Fig. 14 includes an indication of the height of the linear projection of the jet nozzle axis where it intersected the duct exit plane. As can be seen, each jet displacement produced an effect on the exit velocity profile which was slightly exaggerated, relative to the effect which might have been qualitatively estimated on the basis of the shift in the local position of the nozzle axis projection. Consistent with the discussion above, this almost certainly resulted from interaction between the jet and the primary augmentor tube.

Observations of the effects of other, less systematic, variations of jet alignment in the models of both the installed and uninstalled engine facilities, once the primary augmentor tubes had been modified to their shortened configurations, were consistent with the above. Within reasonable limits of misalignment in either the vertical or horizontal planes, the path of the jet core in the augmentor tube did not depart far from the linear projection of the nozzle axis.

Pumping Performance

The cooling flow augmentation ratios measured with unheated air jets in the fully optimized models of the installed and uninstalled engine facilities were 5.99 and 4.97, respectively. These figures could be translated to the full-scale, hot jet situation with the aid of the theory described earlier. As with the earlier calculations, the procedure assumed that the effects of incomplete kinetic and thermal mixing in these relatively long ducts were of second-order importance. In fact, the flow in the isothermal models was some way short of fully mixed although, as evidenced by the typical streamwise static pressure distribution shown in Fig. 15, the rate of pressure rise along the length of the ducts began to level out near the duct exits. Any effect of incomplete mixing in the isothermal models, when using the test results to predict full scale augmentation ratios, should act in the conservative sense—increasing the augmentation ratios in the full-scale facilities rel-

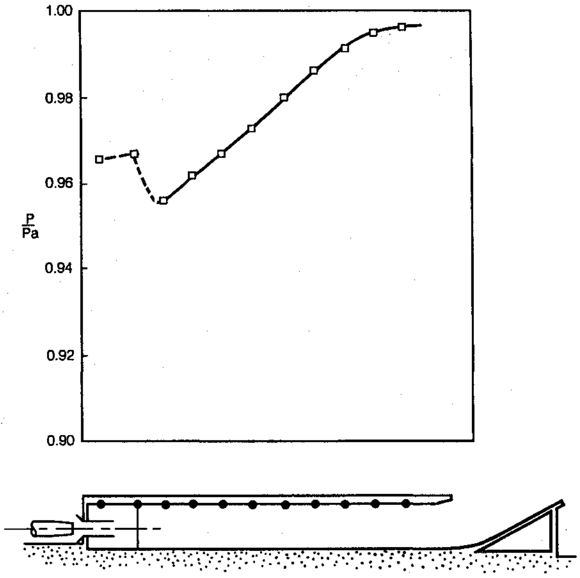

Fig. 15 Static pressure distribution.

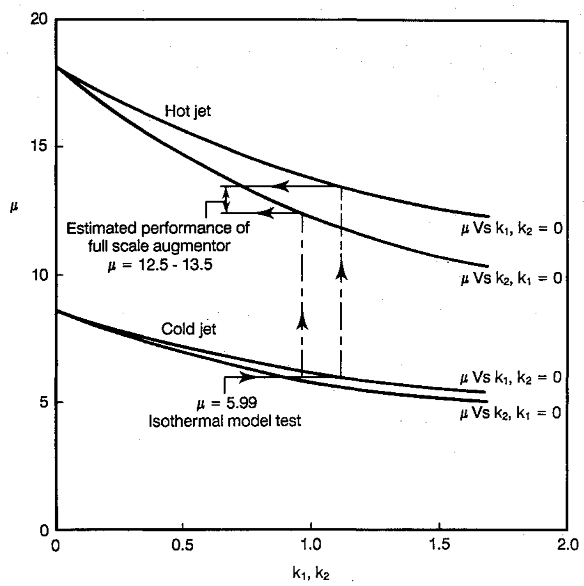

Fig. 16 Estimation of full-scale pumping performance—installed engine facility.

ative to the predicted values—because of the higher rates of mixing which may be expected with hotter jets. As noted earlier, the effects on pumping performance of the small primary augmentor tubes featured in the ultimate designs could safely be ignored.

It was arguably possible to use the static pressures measured in the models to arrive at values for the two loss coefficients, k_1 and k_2, which could in turn be used to calculate the corresponding full-scale augmentor performance. It will be recalled, however, that for theoretical convenience the overall losses for the system were notionally lumped into these two coefficients; while they performed a useful theoretical function, in reality the two coefficients could not therefore be represented by measurable pressure differences. The approach used instead, for the purpose of arriving at loss characteristics which matched the measured pumping performance, was to adopt two possible extremes for apportioning the losses between k_1 and k_2: $k_1 = 0$, with k_2 taking the value necessary to account for the measured performance, and vice-versa.

In Fig. 16, the theoretical value of augmentation ratio in the installed engine facility is plotted against loss coefficient, in two bands: the lower one represents isothermal flow, while the other applies with jet conditions appropriate to the F404 engine in maximum afterburner, including differential gas properties as well as temperature. The upper and lower boundaries of each band correspond to the two extreme combinations of k_1 and k_2 defined above. The experimental value of 5.99 for the isothermal augmentation ratio in the model of the installed engine facility, related to the boundaries of the lower band, defines the limits of the plausible ranges of k_1 and k_2 in the model; when applied in turn to the upper band, these limits indicate that the augmentation ratio for the full-scale facility should be in the range 12.5–13.5. Application of the same procedure to the results relating to the uninstalled engine facility (not shown) arrives at a figure of 10.2–11.3 for that case.

Based on data from experiments with varying jet temperature, Ref. 4 offers a different procedure for correcting pumping performance for the effects of temperature. Applying this to the present isothermal model results yields figures of 14.1 and 11.5, respectively, for augmentation ratios in the full-scale installed and uninstalled engine facilities.

Four points representing the above estimates of full-scale augmentor performance are included in Fig. 4. The values for the installed engine facility are somewhat higher than predictions which might be based on empirical experience with other configurations; however, it should be recalled that they were determined from the highest level of performance recorded during the present model tests, and the models did not have internal surface roughness representative of acoustic linings. It has been observed that this latter effect can account for a 10% difference in pumping performance.[4] The fact that the figures based on the model tests for the uninstalled engine facility look lower against the framework of Fig. 4, may be ascribed to the higher aerodynamic loss associated with the acoustic splitters in the secondary inlets of that configuration.

Observations at Full Scale

Although no detailed flow measurements have been undertaken in the full-scale facilities, observations during their commissioning and during early routine engine run-up operations indicate that the exhaust augmentors function as they were designed to, without any apparent anomolies in flow behavior. Eight thermocouples were mounted in various locations behind the inner skin of the acoustic linings in each of the two main augmentor ducts to provide an indication of lining metal temperature. The maximum temperature which has been registered during max AB operation is 190°C, which is consistent with the mixed gas temperatures associated with the predictions of pumping performance appearing in Fig. 4.

Conclusion

A detailed assessment of the aerothermodynamic designs of the proposed run-up facilities indicated that the designs were sound, subject to certain requirements being observed. Foremost among these were the dimensions of the primary augmentor tubes; these had to be chosen to avoid adverse aerodynamic interactions with the engine jets, which caused distortion of the augmentor duct flow and risked overheating of the duct linings. Other features addressed included the duct exit geometry and the detailed design of the secondary flow inlets.

Measured data from isothermal model tests, coupled with ejector theory, confirmed empirical predictions that the cooling flow pumping performance of the augmentors should comfortably exceed the minimum requirement. The model tests also demonstrated that, given appropriate primary tube dimensions, the augmentor flow was tolerant to both inlet asymmetries and reasonable levels of jet misalignment.

Subsequent observations of the behavior of the full-scale augmentors during engine operation, including measurement of acoustic lining skin temperatures, have indicated that they perform as predicted.

Acknowledgment

Responsibility for the design of the exhaust augmentors rested with the architectural and acoustic design consultant, Challis and Associates Pty., Ltd., contracted by the construction authority, Australian Construction Services, on behalf of the Royal Australian Air Force.

References

[1]Fisher, S. A., and Abdel-Fattah, A. M., "Aerothermodynamic Design Appraisal of Noise Suppressors for F/A-18 Engine Run-Up Facility at RAAF Williamtown," Aeronautical Research Lab., Propulsion Rept. 177, Melbourne, Australia, Oct. 1990.

[2]Fisher, S. A., and Irvine, R. D., "Air Augmentation of Rockets for Low Speed Application," *Proceedings of the Fifth International Symposium on Air Breathing Engines*, Paper 26, Bangalore, India, Feb. 1981, pp. 1–8.

[3]Oran, F. M., and Schiff, M. I., "Design of Air-Cooled Jet Engine Testing Facilities," American Society of Mechanical Engineers, 1979 Israel Joint Gas Turbine Congress, Haifa, Israel, July 1979.

[4]Grunnet, J. L., "An Aerodynamic and Acoustic Test of a 1/15 Scale Model Dry Cooled Jet Aircraft Run-Up Noise Suppression System," FluiDyne Engineering Corp., Minneapolis, MN, 1975.

[5]Quinn, B., "Ejector Performance at High Temperatures and Pressures," *Journal of Aircraft*, Vol. 13, No. 12, 1976, pp. 948–954.

[6]Abdel-Fattah, A. M., "A Theoretical Study of Two-Stage Thrust Augmenting Ejectors," Aeronautical Research Lab., Aero Propulsion Rept. 166, Melbourne, Australia, Nov. 1984.

[7]F404 Status 10 Engine Performance Specification, General Electric Co., Lynn, MA, March 1984.

[8]Grunnet, J. L., and Ference, E., "Model Test and Full-Scale Checkout of Dry-Cooled Jet Runup Sound Suppressors," *Journal of Aircraft*, Vol. 20, No. 11, 1983, pp. 866–871.

[9]Industrial Acoustics Co. Data, New York, April 1983.

[10]Brown, G. L., and Roshko, A., "On Density Effects and Large Structure in Turbulent Mixing Layers," *Journal of Fluid Mechanics*, Vol. 64, Pt. 4, July 1974, pp. 775–816.